Lithuanian Journal of Physics, Vol. **45**, No. 4, pp. 307–315 (2005)

IDENTIFICATION OF CHLOROPHYLL MOLECULES IN PERIPHERAL LIGHT HARVESTING COMPLEX LHC II *

Š. Vaitekonis, G. Trinkūnas, and L. Valkūnas

Institute of Physics, Savanorių 231, LT-02300 Vilnius, Lithuania
E-mail: sarunas@ar.fi.lt

Received 27 June 2005

Chlorophyll site excitation energies of the peripheral plant light-harvesting complex (LHC-II) have been determined by simulating the steady-state absorption and circular dichroism spectra and using new structural data. By applying the genetic algorithm search procedure it has been found that the fit to circular dichroism spectra is critical in narrowing the space of possible solutions. The obtained chlorophyll energy assignment has been verified by the Monte Carlo simulations of the excitation annihilation kinetics. It suggests that the chlorophyll *a* dimers a611-a612, a613-a614, and a602-a603 constitute the sites for the energy migration across the peripheral plant light-harvesting antenna.

Keywords: light-harvesting, LHC-II, genetic algorithm, exciton

PACS: 92.20.Lw, 71.35.-y, 87.15.Aa.

1. Introduction

Light-harvesting and charge separation are the primary processes in photosynthesis. In plants, green algae, and cyanobacteria, the function of harvesting the solar energy is driven by the cooperation of two large protein-cofactor complexes, photosystems I and II, which are located in the thylakoid photosynthetic membranes. Advance in protein-pigment complex refinement techniques enables resolving the structure of both photosystems and their components at high resolution providing crucial data for understanding how high efficiency of photosystems I and II in light capturing and electron transfer is achieved.

LHC-II, the most abundant integral membrane protein of photosystem II in chloroplasts, exists as a trimer and binds half of the thylakoid chlorophyll molecules. The first structure of LHC-II from pea has been determined by electron crystallography at 3.4 Å (4.9 Å) resolution parallel (perpendicular) to the membrane plane [1]. These data revealed some basic structural features of LHC-II, including three transmembrane α-helices (helices A, B, and C) and a short amphipathic helix (helix D), 12 chlorophyll tetrapyrroles with roughly determined locations and orientations, and two carotenoids. A new improved structure of LHC-II from spinach at 2.7 Å resolution has exhibited 14 chlorophylls and unambiguously distinguished them as eight Chl *a* and six Chl *b* molecules [2].

By using the low resolution structural data multiple attempts to explain the spectroscopic results on the basis of the excitonic model have been made in order to achieve the detailed understanding of the functioning of LHC-II. However, this task was too complicated not only because of the low resolution of the crystal structure but also because of the strong overlap of many absorption bands. Therefore, numerous spectroscopic and biochemical experiments were performed in order to reveal the structure–function relationship for LHC-II (see [3] for review). Site-directed mutagenesis studies of the chlorophyll binding residues have determined that five sites are occupied by Chls *a*, three sites by Chls *b*, and four sites can bind both Chl *a* and Chl *b* molecules [4–7]. Several plausible configurations of the antenna including Chl *a*/*b* identities, site energies, and orientations of the 12 Chls were found by modelling the steady-state ant transient absorption (TA) spectra [8–12].

Recent studies of the energy transfer between the chlorophylls using TA and time-resolved fluorescence as well as three pulse photon echo peak shift (3PEPS) and transient grating (TG) measurements have revealed that Chl *b* to Chl *a* transfer is characterized by time constants of 300 and 600 fs at 77 K [13–17] or 150

* The report presented at the 36th Lithuanian National Physics Conference, 16–18 June 2005, Vilnius, Lithuania.

ISSN 1648-8504

and 600 fs at room temperature [13, 18–20] and by a minor 4–9 ps component. Equilibration in the Chl *a* pool occurs within a few hundred femtoseconds, but at blue side excitation the slow picosecond components are also observed [14, 16]. Even more complex excitation energy relaxation channels are developed while simultaneously fitting the steady-state spectra, including absorption (OD) and linear dichroism (LD), TA, TG, and 3PEPS kinetics, with the Redfield relaxation theory [10, 21–24].

Using new structural data a new exciton model of the LHC-II trimer with specific site energies has been proposed [25]. It has been shown that the fast Chl *b*→Chl *a* transfer is determined by a link of the Chls *b* to strongly coupled Chl *a* clusters. Long-lived (3–12 ps) components of the energy transfer kinetics are determined by a very slow flow of energy from the so-called monomeric bottleneck sites to the Chl *a* clusters. The dynamics in the Chl *a* region is determined by a fast (100–300 fs) exciton relaxation, the slower (300–800 fs) migration between these clusters, and a very slow transfer to the quasi-equilibrated Chl *a* sites located on the outer side of the trimeric LHC-II complex.

It is important to note that a variety of the energy transfer time scales stems from the inhomogeneity of Chl site excitation energies. However, the assignment of kinetic components to individual Chl molecules or their clusters is problematic as many dissimilar excitation energy assignments may result in similar simulated kinetics. Firstly, the uniqueness of the Chl site energy assignments remains an open issue because the simulation of kinetic data is a costly procedure disabling the test of the statistically meaningful number of assignments. Secondly, the kinetic data can be potentially subjected to the exciton–exciton annihilation altering the Chl spectral properties.

In this paper we focus on exhaustive searching for Chl transition energies of the trimeric LHC-II light-harvesting complex by a genetic algorithm (GA) using the new crystal structure [25] and exciton modelling of OD and circular dichroism (CD) spectra at room temperature. Usage of the steady state spectra for the fitting criterion enables the testing of as large as possible set of different assignments. Inclusion of the CD spectrum into the fitting criterion makes the fitting task favourably different from that in the recent Chl assignment studies. The rotational polarization is very sensitive to the excitonic interaction and therefore significantly narrows the space of possible solutions. The Monte Carlo simulation of the transient absorption spectra under the exciton–exciton annihilation conditions serves as a dynamic validation criterion of the Chl assignment. The most likely assignments are compared to the recently obtained model [25] based on the combined steady-state spectra and kinetic simulations.

2. Model and methods

2.1. Exciton spectra

To expose the excitonic effect on the long wavelength spectrum we will relate the transition energy of each Chl molecule to the two-level scheme determining the electronic ground (ϕ_i^0) and excited (ϕ_i^*)states of the ith molecule with characteristic energies ε_i^0 and ε_i^*, respectively. The exciton Hamiltonian of the system in the Heitler–London approximation thus can be presented accordingly [26]:

$$H_{ex} = \sum_i \varepsilon_i |i\rangle\langle i| + \sum_{i,j(j\succ i)} \left(W_{ij}|i\rangle\langle j| + W_{ji}|j\rangle\langle i|\right), \tag{1}$$

where $\varepsilon_i = \varepsilon_i^* - \varepsilon_i^0$ corresponds to the excitation energy of the ith molecule,

$$|i\rangle = \phi_i^* \prod_{j\neq i} \phi_i^0 \tag{2}$$

is the wave function for the excitation situated on the ith molecule, W_{ij} is the matrix element of the resonance interaction between the ith and jth molecules. The Chl–Chl intermolecular distances in LHC-II exceed 8 Å [2], thus, the overlap of molecular wave functions is negligible and therefore the electron exchange effect in the intermolecular interaction can be neglected. In this case the dipole–dipole approximation determining the interaction between two point-dipoles separated by the distance R can be used:

$$W_{ij} = C\left(\frac{\overrightarrow{\mu}_i \cdot \overrightarrow{\mu}_j}{R^3} - \frac{3(\overrightarrow{\mu}_i \cdot \overrightarrow{R})(\overrightarrow{\mu}_j \cdot \overrightarrow{R})}{R^5}\right), \tag{3}$$

where $\overrightarrow{\mu}_i$ is the vector of the transition dipole moment of the ith molecule, C is the parameter determining the local field effect as well as the numerical relationship between the energy scale for the matrix element and the strength scale for the transition dipole moment [26]. Thus, for interacting molecules of the same type we get:

$$W_{ij} = 5.04 \cdot C\frac{kd}{R^3}, \tag{4}$$

where

$$k = \cos(\widehat{\mu_i} \cdot \widehat{\mu_j}) - 3\cos\left(\widehat{\mu_i} \cdot \widehat{R}\right)\cos\left(\widehat{\mu_j} \cdot \widehat{R}\right) \tag{5}$$

Table 1. Gaussian decomposition of Chl *a* and Chl *b* line contour spectra [1].

	Chl *a*			Chl *b*		
#	x	w	A	x	w	A
1	–11	–14792	0.6871	–11	–51200	0.806
2	111	–123008	0.3505	209	–188498	0.2449
3	1098	–102152	0.1068	1308	–217800	0.2255

is the orientation factor, $\widehat{\mu}$ and $\widehat{R}$ determine the corresponding unit-vectors, and $d = |\mu|^2$ is the dipole strength of the molecular transition. The dipole moment of the longest wavelength transition of the Chl molecules is oriented almost along the line connecting N_{II} and N_{IV} atoms in the chlorine plane [27]. C takes into account the influence of the medium and is given by $C = (n^2 + 2)^2/9n^2$ [26]. By neglecting the specificity of the protein surrounding of Chls for W_{ij} given in cm^{-1} and d in Debye^2, we can assume that $n = 1.5$ (this gives $C = 0.89$) and $d = 21.5$ Debye^2 [28].

The excitonic OD and CD spectra have been calculated by using the eigenenergies and eigenvectors of the Hamiltonian as given in Eq. (1) and following the conventional expressions [26]. Direct diagonalization of the exciton Hamiltonian taking into account the structural arrangement data of the Chl molecules in LHC-II allowed us to obtain the stick-type energy spectrum. As most of Chls of both types *a* and *b* are weakly excitonically coupled, it is reasonable to assume that the convolution of the latter with the line contours of Chl *a* and Chl *b* molecules (Table 1) obtained using mutant LHC-II proteins lacking one Chl *a* or Chl *b* molecule [29] comprises the model spectrum that can be compared with the absorption spectrum measured at room temperature. Assuming that the inhomogeneous distribution is the same for all the Chls, these profiles are expected to properly take into consideration the local inhomogeneous distribution of the Chl site. Then the main fitting parameters are the positions of the absorption spectra of all Chls. For the spectrally homogeneous model the transition energies appear to be at 674 nm for all Chl *a* and at 655 nm for all Chl *b* molecules. The calculated OD and CD spectra using the spectrally homogeneous model do not fit properly the corresponding experimental spectra [30] (Fig. 1, dotted lines) suggesting that further steps in improvement of the calculated spectra are required. Further on we will assume that molecular transition energies of all Chls in the LHC-II monomer are different.

2.2. Evolutionary search for the Chl transition energies

The trimeric LHC-II complex binds 42 Chl pigments. To find transition energy for each Chl molecule one has to delve into multidimensional space of search (the number of dimensions is equal to the number of Chl molecules in the complex), which is unpredictable in terms of continuity and the derivative existence, and contains a huge number of possibilities as well. To find an answer in space with such properties, the search procedure with capabilities of parallel exploration of the multidimensional space and blindness to auxiliary information is needed. The genetic algorithm developed by Holland [31] is the most suitable search procedure that meets these requirements. A similar application of the genetic algorithm in search for transition energies of photosystem I core complex has been recently presented [32]. Here we employ a simple genetic algorithm [33].

Practical realization of the algorithm begins with the binary encoding of the excitation wavelength variance for single Chl. Wavelengths are allowed to vary from 638 to 702 nm (638–659 nm for Chl *b* and 660–702 nm for Chl *a*) with the step of 1 nm comprising 64 different values. To encode a given range, 6 bits of information, also called a gene, are needed. Thus, to encode the excitation wavelengths of all Chls of the LHC-II, the string of 14 genes, also called a chromosome, is composed.

A stochastic tournament implementation of the reproduction operator was used. It is based on a random selection of two strings from the old population with subsequent duel for participation in a mating process. A duel process is controlled by a selection factor – a constant that determines the probability for the string with better fitness to win the tournament. If the uniform random number generated from the interval $[0; 1]$ is smaller than the selection factor, the winner is one with better fitness. As mating occurs in pairs and the reproduction operator returns a single parent; to produce a pair of mating strings it has to be called twice. During the fitness-dependent reproduction cycle, when the value of the selection factor is larger than 0.5, strings with higher fitness have a larger number of offsprings in the succeeding generation.

Each string randomly seeded with 14 binary coded excitation wavelength values represents a trimeric LHC-II complex (or solution). Code alterations of each string by genetic operations during an evolutionary process occur according to the fitness of the individual

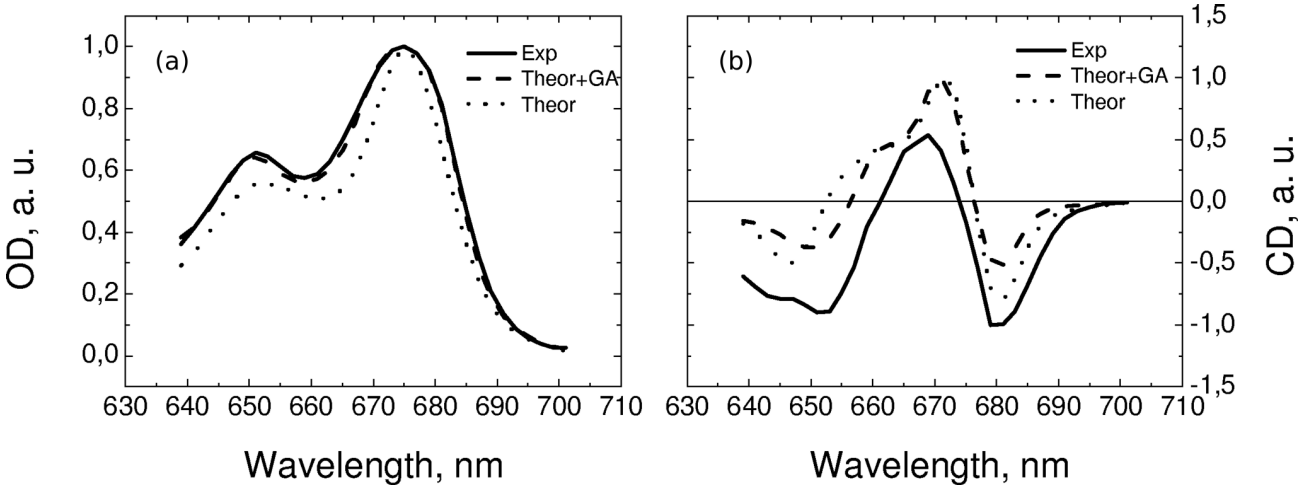

Fig. 1. Comparison of (a) OD and (b) CD spectra of the trimeric LHC-II complex calculated assuming the transition wavelengths for all Chl *a* molecules to be at 674 nm and for Chl *b* molecules at 650 nm (dotted line) with corresponding spectra as obtained by the genetic algorithm search (dashed line). The exiton stick spectra are dressed with line contours of Chl *a* and Chl *b* molecules presented in Table 1. Experimental data (solid line) are taken from [30].

string. To evaluate fitness, the string undergoes a decoding procedure. The decoded string, also called an individual, consisting of 14 Chl excitation wavelengths (energies) is substituted into the Hamiltonian determined by Eq. (1) and the diagonalization of the latter is performed. By using the eigenvalues and eigenvectors the OD and CD spectra are calculated. The LD spectrum calculations can also be easily added. The obtained stick spectra are dressed with line contours of single Chl *a* and Chl *b* molecules as described above. The χ^2 criterion is finally used to estimate the deviation of the simulated OD and CD spectra from the experimental data and serves for the solution fitness or the payoff.

Genetic algorithm parameters. The population size was 10000. To reach the convergence of search, from 100 to 200 generations were needed. The optimal selection factor, crossover and mutation probabilities were found to be about 0.8–0.9, 0.8, and 0.008–0.01, respectively.

The Chl excitation energy assignment corresponding to the best fit obtained by the genetic algorithm search is presented in Table 2 and Fig. 2. The newly calculated OD and CD spectra are presented in Fig. 1 by dashed lines. The theoretical OD spectrum fits the experimental one very well. The simulated CD spectrum follows the shape of the experimental spectrum, however showing a systematic shift on a vertical axis. This can be related to the intrinsic rotational activity of the Chls [34] that has not been taken into account.

2.3. Validation of GA search results. Exciton–exciton annihilation dynamics

Calculations of the transient absorption spectrum were based on the one-dimensional annihilation (coagulation) model with periodic boundary conditions for nearest-neighbour type interactions [35, 36]. To simulate the process of a real system the basic model was extended into the three-dimensional model with neighbour–neighbour type interactions.

The dynamics of the system was determined by the rates $\Gamma^{\alpha,\beta}_{\gamma,\delta}$ for the neighbour–neighbour interactions:

$$(\alpha,\beta) \rightarrow (\gamma,\delta)\,.$$

Here a value of $\alpha,\beta,\gamma,\delta,= 1$ corresponds to an excited Chl molecule and a value of 0 to a Chl molecule in the ground state. In an initial state every Chl molecule of the trimeric LHC-II complex is excited with equal probability p at $t = 0$. We denote a discrete time step by Δt. The value of Δt must be chosen so that $\max\left(\Gamma^{\alpha,\beta}_{\gamma,\delta}\right)\cdot\Delta t \leq 1$.

Each Monte Carlo step consists of the following operations:

1. An excited Chl molecule is chosen at random and afterward, by playing the roulette wheel game, is situated on one of its neighbours. To play the roulette wheel game the wheel must be divided into parts. The number of parts is equal to the number

Table 2. Transition wavelengths for all Chl molecules of the trimeric LHC-II complex.

#	b601	a602	a603	a604	b605	b606	b607	b608	b609	a610	a611	a612	a613	a614
nm	659	673	674	661	639	659	659	656	659	671	672	675	673	680

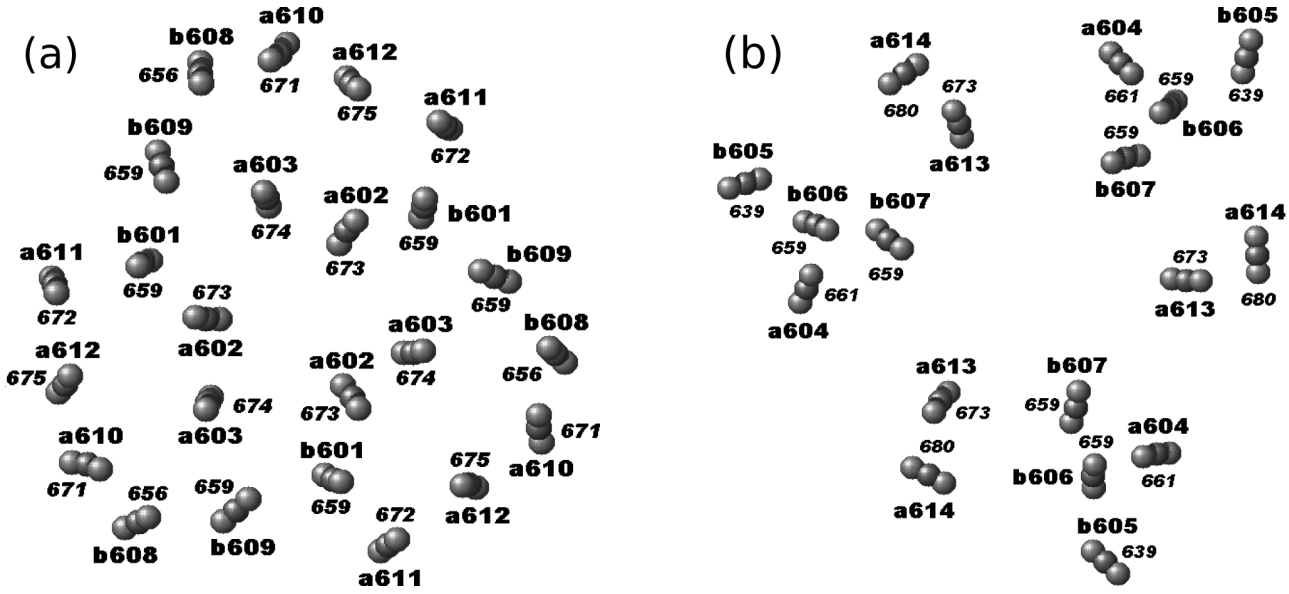

Fig. 2. Arrangement of chlorophylls within two layers in the trimeric LHC-II complex: (a) the stromal side, (b) the lumenal side. Three atoms represent chlorophylls: the central magnesium atom and two nitrogen atoms. The connecting line between the two nitrogens defines the directions of the Q_y transition dipole. Alphanumerical notes identify Chl molecules according to the structure file 1RWT [2]. The smaller italic numerical notes correspond to transition wavelengths of chlorophylls.

of neighbours that the chosen molecule α has. The size of each part is equal to

$$x_{j;j\neq\alpha} = \Gamma^{\alpha,j}_{\gamma,\delta}\frac{1}{N-1}\sum_{i=1;i\neq\alpha}^{N-1}\Gamma^{\alpha,i}_{\gamma,\delta}\,. \qquad (6)$$

Here N is the number of molecules in the trimeric LHC-II complex and $N-1$ is the number of neighbours of the α molecule. Then the random number from interval $[0;1]$ is generated. Values of x_j are summed until the resulting sum becomes larger than the random number. The index of the last added $x_j$value is declared as neighbour of the α molecule.

2. New configuration $(\gamma,\delta)\neq(\alpha,\beta)$ is chosen with the probability $n(\alpha,\beta)\Gamma^{\alpha,\beta}_{\gamma,\delta}\Delta t$ or the pair remains unchanged with probability

$$1-n(\alpha,\beta)\Delta t\sum_{(\gamma,\delta)\neq(\alpha,\beta)}\Gamma^{\alpha,\beta}_{\gamma,\delta}\,.$$

Here $n(\alpha,\beta)$ is defined by

$$n(\alpha,\beta)=\begin{cases}1 & \text{if} \quad (\alpha,\beta)=(1,1)\\ 2 & \text{if} \quad (\alpha,\beta)=(1,0)\\ 2 & \text{if} \quad (\alpha,\beta)=(0,1)\end{cases}\,.$$

3. Finally, the time is increased, $t\rightarrow t+\Delta t/N_{\rm e}$, where $N_{\rm e}$ is the total number of the excited Chl molecules in the trimeric LHC-II complex. The given model was successfully tested using the one-dimensional string of the variable length under periodic boundary conditions [36].

For the Monte Carlo simulations of the real system dynamics the rate constants for energy transfer from a donor pigment j to an acceptor pigment i were calculated according to the Förster formula [37]:

$$W_{i\leftarrow j}=\frac{9000(\ln 10)k^2_{ij}}{128\pi^5 n^4 N_{\rm A}\tau_{0j}R^6_{ij}}\int\limits_0^\infty f_j(\omega)\xi_i(\omega)\frac{{\rm d}\omega}{\omega^4}\,. \quad (7)$$

In this formula ω denotes the wavenumber (cm^{-1}), $f_j(\omega)$ is the fluorescence spectrum of the donor pigment with area normalized to unity, and $\xi_i(\omega)$ is the molar decadic extinction coefficient of the acceptor

molecule. $N_{\rm A}$ is the Avogadro number, n is the refractive index of the surrounding medium, and τ_{0j} is the radiative lifetime (ns) of the donor. The energy transfer rate depends on the distance R_{ij} between the pigments and on the orientation factor k_{ij} (see Eq. (5)).

To fulfil the detailed balance condition, back-transfer rates returned by the Förster Eq. (7) are multiplied by the Boltzmann factor. If the transition energy of the donor pigment ε_j (cm^{-1}) is lower than transition energy of the acceptor pigment ε_i (cm^{-1}), the constant of the back-transfer is calculated accordingly as

$$W_{i\leftarrow j}^{\rm new} = W_{i\leftarrow j}^{\rm old} \exp\left(- \frac{\varepsilon_i - \varepsilon_j}{k_{\rm B} \cdot T} \right), \qquad (8)$$

where T is the temperature.

To validate results obtained after the evolutionary search procedure, Monte Carlo simulation [38] of the transient absorption spectra of the trimeric LHC-II complex was performed. To obtain good agreement with the experimental data, the value of the refractive index n was set to 2.5. The simulated transient absorption spectrum of the trimeric LHC-II complex is presented in Fig. 3. Monte Carlo simulations of the transient absorption spectrum of the trimeric LHC-II complex assume that the given number of exitations are populated on pigments instantaneously. In reality the excitation of the system is achieved using a pulse, which is not infinitesimally short, but has the duration of about 6 ps. During this period of time two opposite processes take place: a gradual excitation of the LHC-II complex and fast annihilation of newly formed excitations. The disagreement between the simulated results and the experimental data at the very early phase of transient absorption spectra is clear (see Fig. 3). After about 7 ps the influence of the excitation pulse duration vanishes and a good agreement with the experimental data is achieved. It suggests that the GA determined values of Chls transition energies are rather reliable.

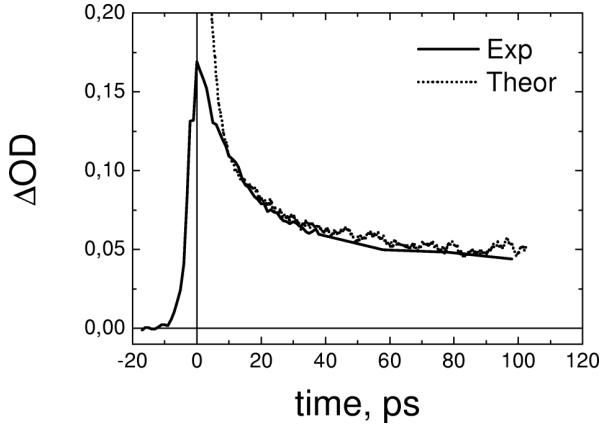

Fig. 3. Transient absorption spectrum of the trimeric LHC-II complex at 682 nm and $T = 290$ K simulated by the Monte Carlo method (dotted line). Experimental data (solid line) are taken from Fig. 5 of [39]. Excitation intensity 0.1.

3. Discussion and conclusions

Knowledge of the structural organization of the pigment molecules in the LHC-II complex provides the possibility of calculating the excitation energy spectrum by using various theoretical approaches. As demonstrated in Figs. 1(a) and (b), calculation of the exciton spectrum by assuming the homogeneous transition energies for all Chl *a* and Chl *b* pigments and the same refractive index by estimating the matrix elements of the resonance interaction does not fit the experimental OD and CD spectra. Inhomogeneity of the transition energy distribution (diagonal distribution of the molecular transition energies) substantially improves the possibility of fitting the OD spectrum (Fig. 1(a)). The simulated CD spectrum (Fig. 1(b)) still shows the systematic shift on the vertical axis relative to the experimental one. However, it can be accounted for by taking into consideration the intrinsic Chl rotational strength [34].

The use of the GA search enables testing a multitude of the possible Chl excitation energy assignments. When fitting the OD spectrum only, the number of relevant Chl energy assignments is very large (up to 1000). This set also includes the assignment similar to one recently obtained [25]. It is clear because the OD, LD, and steady-state fluorescence spectra with subsequent selection of the final assignment to fit the kinetic data were used by these authors for the fit criterion. However, including CD into the fit criterion introduces much stronger constraint on the orientations of Chls which is indeed critical. The number of the relevant assignments is reduced to just a few, very similar to one presented in Fig. 2. Note that the previous assignment [25] does not properly follow the CD spectrum although it only slightly differs from the one obtained by us (for comparison see Fig. 4).

Three lowest states (in the limits of the thermal energy at room temperature) localized on sites a611–a612, a613–a614, and a602–a603 are close to the attribution as obtained in [25] (a610–a611–a612, a602–a603, and a613–a614). These sites of exciton localization are of great importance because they constitute the superlattice for the excitation energy migration across the peripheral light-harvesting antenna.

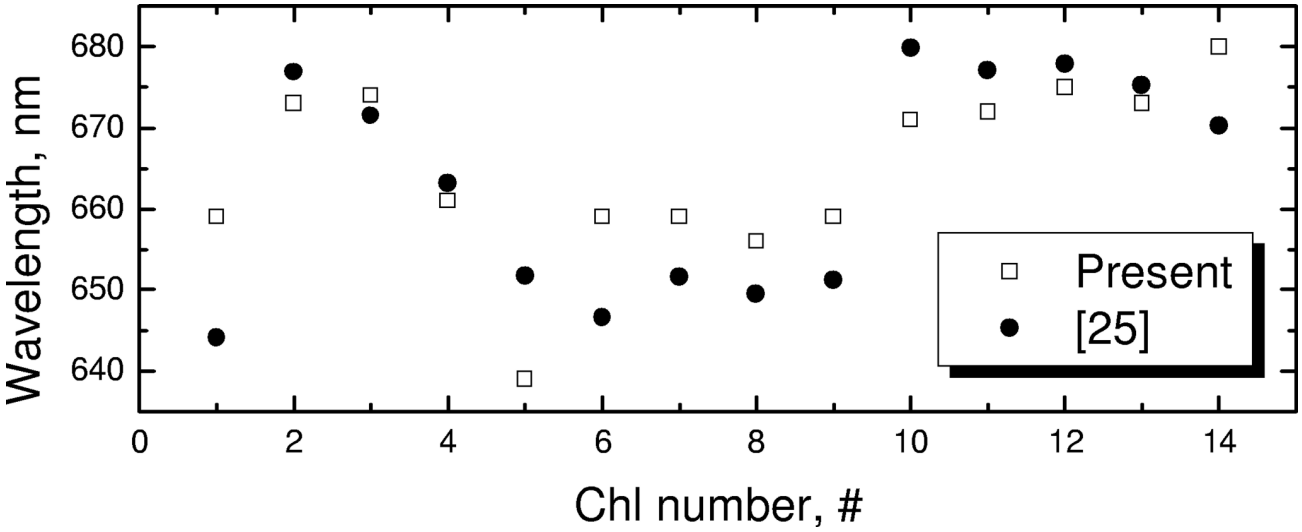

Fig. 4. Comparison of the obtained Chl site excitation energies (maxima of absorption spectra) to ones from [25]. Reference data [25] comprising the positions of the zero phonon lines are shifted by 330 cm^{-1} for better view.

The validation of the obtained Chl excitation energy assignment has been performed by simulating the exciton–exciton annihilation kinetics measured at 682 nm. Due to a particularly low excitation wavelength the relevance of the excitation energies of Chls *a* has been verified.

The disagreement between the refractive index values while simulating the steady-state ($n = 1.5$) and transient absorption ($n = 2.5$) spectra is obtained. To calculate the spectral overlap integrals for the Förster transfer rates the Chl spectral shapes obtained from the mutant LHC-II proteins lacking one Chl *a* or Chl *b* molecule [29] have been used. However, these experimentally obtained spectral shapes consist of a homogeneous profile convoluted with the site inhomogeneous distribution function. Broader spectra overestimate the obtained overlap integrals. Therefore, by applying a higher refractive index the transfer rates have been properly rescaled. This suggests that the refractive index relevant for LHC-II should be less than 2.5.

The final energy distribution by no means is determined by the reliability of the experimental data used for fitting. Spectra collected from different kind of sources (different kind of species of the host organism) and measured under different conditions make results of calculations less reliable. Moreover, the nature of the GA does not allow finding an accurate answer because of the limited resolution of the space of encoded parameters and randomness in the basic operators used. Therefore every set of Chl transition energies returned by the GA contains uncertainties that add up to the reliability issues of the experimental data. However, the GA is a powerful search tool that does not require any auxiliary information or huge computation power and is capable of finding solution in multidimensional space in a relatively short time. For the problems of such complexity it is the most suitable tool with acceptable level of inaccuracy.

Acknowledgement

This research was supported by the Lithuanian State Science and Studies Foundation.

References

[1] W. Kühlbrandt, D.N. Wang, and Y. Fujiyoshi, Atomic model of plant light-harvesting complex by electron crystallography, Nature **367**, 614–621 (1994).

[2] Z. Liu, H. Yan, K. Wang, T. Kuang, J. Zhang, L. Gui, X. An, and W. Chang, Crystal structure of spinach major light-harvesting complex at 2.72 Å resolution, Nature **428**, 287–292 (2004).

[3] H. van Amerongen and R. van Grondelle, Understanding the energy transfer function of LHCII, the major light-harvesting complex of green plants, J. Phys. Chem. B **105**, 604–617 (2001).

[4] R. Remelli, C. Varotto, D. Sandona, R. Croce, and R. Bassi, Chlorophyll binding to monomeric light-harvesting complex. A mutation analysis of chromophore-binding residues, J. Biol. Chem. **274**, 33510–33521 (1999).

[5] H. Rogl and W. Kühlbrandt, Mutant trimers of light-harvesting complex II exhibit altered pigment content and spectroscopic features, Biochemistry **38**, 16214–16222 (1999).

[6] C. Yang, K. Kosemund, C. Cornet, and H. Paulsen, Exchange of pigment-binding amino acids in light-

harvesting chlorophyll a/b protein, Biochemistry **38**, 16205–16213 (1999).

[7] H. Rogl, R. Schödel, H. Lokstein, W. Kühlbrandt, and A. Schubert, Assignment of spectral substructures to pigment-binding sites in higher plant light-harvesting complex LHC-II, Biochemistry **41**, 2281–2287 (2002).

[8] Th. Renger and V. May, Simulations of frequency domain spectra: Structure–function relationships in photosynthetic pigment–protein complexes, Phys. Rev. Lett. **84**, 5228–5231 (2000).

[9] E.I. Iseri and D. Gülen, Chlorophyll transition dipole moment orientations and pathways for flow of excitation energy among the chlorophylls of the major plant antenna, LHCII, Eur. Biophys. J. **30**, 344–353 (2001).

[10] V. Novoderezhkin, J.M. Salverda, H. van Amerongen, and R. van Grondelle, Exciton modeling of energy-transfer dynamics in the LHCII complex of higher plants: A Redfield theory approach, J. Phys. Chem. B **107**, 1893–1912 (2003).

[11] V. Novoderezhkin, M. Palacios, H. van Amerongen, and R. van Grondelle, Energy-transfer dynamics in the LHCII complex of higher plants: Modified Redfield approach, J. Phys. Chem. B **108**, 10363–10375 (2004).

[12] G. Trinkunas, J.P. Connelly, M.G. Müller, L. Valkunas, and A.R. Holzwarth, Model for the excitation dynamics in the light-harvesting complex II from higher plants, J. Phys. Chem. B **101**, 7313–7320 (1997).

[13] T. Bittner, G.P. Wiederrecht, K.-D. Irrgang, G. Renger, and M.R. Wasielewski, Femtosecond transient absorption spectroscopy on the light-harvesting Chl *a*/*b* protein complex of photosystem II at room temperature and 12 K, Chem. Phys. **194**, 311–322 (1995).

[14] H.M. Visser, F.J. Kleima, I.H.M. van Stokkum, R. van Grondelle, and H. van Amerongen, Probing the many energy-transfer processes in the photosynthetic light-harvesting complex II at 77 K using energy-selective sub-picosecond transient absorption spectroscopy, J. Chem. Phys. **210**, 297–312 (1996).

[15] F.J. Kleima, C.C. Gradinaru, F. Calkoen, I.H.M. van Stokkum, R. van Grondelle, and H. van Amerongen, Energy transfer in LHCII monomers at 77 K studied by sub-picosecond transient absorption spectroscopy, Biochemistry **36**, 15262–15268 (1997).

[16] C.C. Gradinaru, S. Özdemir, D. Gülen, I.H.M. van Stokkum, R. van Grondelle, and H. van Amerongen, The flow of excitation in LHCII monomers. Implications for the structural model of the major plant antenna, Biophys. J. **75**, 3064–3077 (1998).

[17] C.C. Gradinaru, I.H.M. van Stokkum, A.A. Pascal, R. van Grondelle, and H. van Amerongen, Identifying the pathways of energy transfer between carotenoids and chlorophylls in LHCII and CP29. A multicolor, femtosecond pump-probe study, J. Phys. Chem. B **104**, 9330–9342 (2000).

[18] M. Du, X. Xie, L. Mets, and G.R. Fleming, Direct observation of ultrafast energy-transfer processes in light-harvesting complex II, J. Phys. Chem. **98**, 4736–4741 (1994).

[19] T. Bittner, K.-D. Irrgang, G. Renger, and M.R. Wasielewski, Ultrafast excitation energy transfer and exciton–exciton annihilation processes in isolated light-harvesting complexes of photosystem II (LHC-II) from spinach, J. Phys. Chem. **98**, 11821–11826 (1994).

[20] J.P. Connelly, M.G. Müller, M. Hucke, G. Gatzen, C.W. Mullineaux, A.V. Ruban, P. Horton, and A.R. Holzwarth, Ultrafast spectroscopy of trimeric light-harvesting complex II from higher plants, J. Phys. Chem. B **101**, 1902–1909 (1997).

[21] R. Agarwal, B.P. Krueger, G.D. Scholes, M. Yang, J. Yom, L. Mets, and G.R. Fleming, Ultrafast energy transfer in LHC-II revealed by three-pulse photon echo peak shift measurements, J. Phys. Chem. B **104**, 2908–2918 (2000).

[22] J.M. Salverda, M. Vengris, B.P. Krueger, G.D. Scholes, A.R. Czarnoleski, V. Novoderezhkin, H. van Amerongen, and R. van Grondelle, Energy transfer in light-harvesting complexes LHCII and CP29 of spinach studied with three-pulse echo peak shift and transient grating, Biophys. J. **84**, 450–465 (2003).

[23] A.G. Redfield, The theory of relaxation processes, Adv. Magn. Reson. **1**, 1 (1965).

[24] W.T. Pollard, A.K. Felts, and R.A. Friesner, The Redfield equation in condensed phase quantum dynamics, Adv. Chem. Phys., XCIII, 77, *New Methods in Computational Mechanics*, eds. I. Prigogine and S.A. Rice (ISBN: 0-471-19127-2, 1996).

[25] V.I. Novoderezhkin, M.A. Palacios, H. van Amerongen, and R. van Grondelle, Excitation dynamics in the LHCII complex of higher plants: Modeling based on the 2.72 crystal structure, J. Phys. Chem. B **109**, 10493–10504 (2005).

[26] H. van Amerongen, L. Valkunas, and R. van Grondelle, *Photosynthetic Excitons* (World Scientific Co., Singapore, 2000).

[27] M.A.M.J. van Zandvoort, D. Wrobel, P. Lettinga, G. van Ginkel, and Y.K. Levine, The orientation of the transition dipole moments of chlorophyll *a* and pheophytin *a* in their molecular frame, Photochem. Photobiol. **62**, 299–308 (1995).

[28] R.S. Knox, and H. van Amerongen, Refractive index dependence of the Förster resonance excitation transfer rate, J. Phys. Chem. B **206**, 5289–5293 (2002).

[29] G. Cinque, R. Croce, and R. Bassi, Absorption spectra of chlorophyll *a* and *b* in Lhcb protein environment, Photosynth. Res. **64**, 233–242 (2000).

[30] A.V. Ruban, F. Calkoen, S.L.S. Kwa, R. van Grondelle, P. Horton, and J.P. Dekker, Characterisation of LHC-II in the aggregated state by linear and circular dichroism spectroscopy, Biochim. Biophys. Acta **1321**, 61–70 (1997).

[31] J.H. Holland, *Adaptation in Natural and Artificial Systems* (University of Michigan Press, Ann Arbor, 1975).
[32] S. Vaitekonis, G. Trinkunas, and L. Valkunas, Red chlorophylls in the exciton model of Photosystem I, Photosynth. Res. (2005) (in press).
[33] D.E. Goldberg, *Genetic Algorythms in Search, Optimization, and Machine Learning* (Addison–Wesley, Reading, Massachusetts, 1989).
[34] C. Houssier and K. Sauer, Circular dichroism and magnetic circular dichroism of the chlorophyll and protochlorophyll pigments, J. Am. Chem. Soc. **92**(4), 779–791 (1970).
[35] K. Krebs, M.P. Pfannmuller, B. Wehefritz, and H. Hinrichsen, Finite-size scaling studies of one-dimensional reaction-diffusion systems. Part I. Analytical results, J. Stat. Phys. **78**, 1429–1470 (1995).
[36] K. Krebs, M.P. Pfannmuller, H. Simon, and B. Wehefritz, Finite-size scaling studies of one-dimensional reaction-diffusion systems. Part II. Numerical methods, J. Stat. Phys. **78**, 1471–1491 (1995).
[37] Th. Forster, in: *Modern Quantum Chemistry*, Part II, ed. O. Sinanoglu (Academic Press, New York 1965).
[38] J.M. Hammersley and D.C. Handscomb, *Monte Carlo Methods* (Methuen, London, 1964).
[39] V. Barzda, V. Gulbinas, R. Kananavicius, V. Cervinskas, H. van Amerongen, R. van Grondelle, and L. Valkunas, Singlet–singlet annihilation kinetics in aggregates and trimers of LHCII, Biophys. J. **80**, 2409–2421 (2001).

CHLOROFILO MOLEKULIŲ IDENTIFIKACIJA PERIFERINIAME ŠVIESĄ SURENKANČIAME KOMPLEKSE LHC II

Š. Vaitekonis, G. Trinkūnas, L. Valkūnas

Fizikos institutas, Vilnius, Lietuva

Santrauka

Modeliuojant nuostoviuosius sugerties ir cirkuliarinio dichroizmo spektrus, panaudojus naujus struktūrinius duomenis, įvertintos periferinio šviesą surenkančio komplekso (LHC-II) chlorofilo molekulių sužadinimo energijos. Taikant genetinio algoritmo paieškos procedūrą, pastebėta, kad sprendinių paieškos erdvę labiausiai siaurina teorinio ir eksperimentinio cirkuliarinio dichroizmo spektrų sutapimas. Rastos chlorofilo molekulių sužadinimo energijos vertės patikrintos Monte Carlo metodu modeliuojant sužadinimo anihiliacijos kinetikos būdus. Pastebėta, kad chlorofilo *a* molekulių dimerai a611–a612, a613–a614 ir a602–a603 yra mazgai, kuriais periferinėje šviesą surenkančioje antenoje vyksta energijos migracija.